Supporting Information

Four one-dimensional lanthanide-phenylacetate polymers exhibiting luminescence and magnetic cooling/spin-glass behavior

Zhong-Yi Li, Ya-Lan Xu, Xiang-Fei Zhang, Bin Zhai,* Fu-Li Zhang, Jian-Jun Zhang,* Chi Zhang, Su-Zhi Li and Guang-Xiu Cao*

Table S1. Selected bond lengths (Å) and angles (°) for **2**.

Gd(1)-O(3)	2.322(3)	Gd(1)-O(2)#2	2.490(2)
Gd(1)-O(1)	2.400(2)	Gd(1)-O(1)#2	2.512(2)
Gd(1)-O(4)#2	2.421(3)	Gd(1)-C(1)#2	2.881(3)
Gd(1)-O(5)	2.441(4)	Gd(1)-Gd(1)#4	4.06120(15)
Gd(1)-O(1)-Gd(1)#4	111.53(8)	O(3)-Gd(1)-O(1)	76.25(9)
O(1)#1-Gd(1)-O(2)#2	138.36(8)	O(3)-Gd(1)-O(1)#2	127.18(8)
O(1)#1-Gd(1)-O(4)#2	76.36(8)	O(3)-Gd(1)-O(2)#2	83.94(7)
O(1)#3-Gd(1)-O(1)#2	65.13(10)	O(3)-Gd(1)-O(2)#3	83.94(7)
O(1)-Gd(1)-O(1)#1	68.55(10)	O(3)-Gd(1)-O(4)#2	146.70(11)
O(1)-Gd(1)-O(1)#2	107.78(7)	O(3)-Gd(1)-O(5)	71.60(12)
O(1)-Gd(1)-O(1)#3	155.74(2)	O(4)#2-Gd(1)-O(1)#2	79.48(8)
O(1)-Gd(1)-O(2)#2	71.34(8)	O(4)#2-Gd(1)-O(2)#2	104.71(7)
O(1)-Gd(1)-O(5)	132.53(8)	O(4)#2-Gd(1)-O(5)	141.70(12)
O(2)#2-Gd(1)-O(1)#2	51.43(7)	O(5)-Gd(1)-O(1)#2	68.49(9)
O(2)#2-Gd(1)-O(1)#3	113.36(7)	O(5)-Gd(1)-O(2)#2	71.36(7)
O(2)#3-Gd(1)-O(2)#2	142.71(14)		

Symmetry codes: #1 x, -y+1/2, z; #2 x-1/2, y, -z+3/2; #3 x-1/2, -y+1/2, -z+3/2; #4 x+1/2, y, -z+3/2.

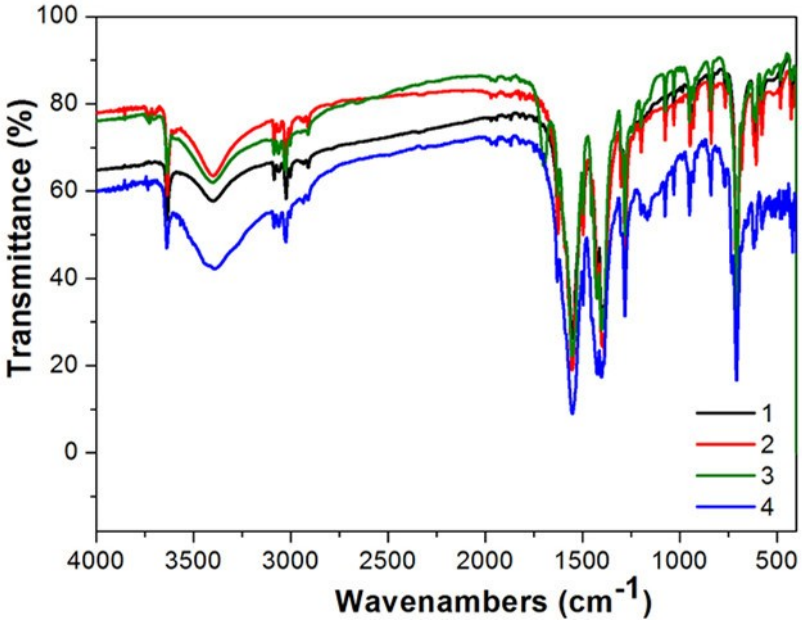

Fig. S1 The IR spectra of **1-4**.

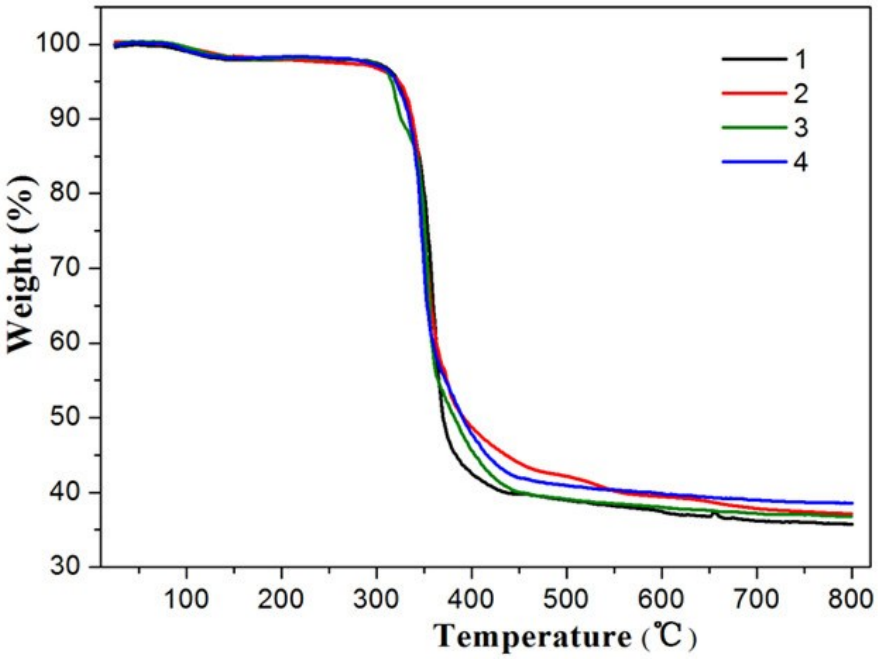

Fig. S2 TG curves for **1-4** in a nitrogen atmosphere (10 °C/min).

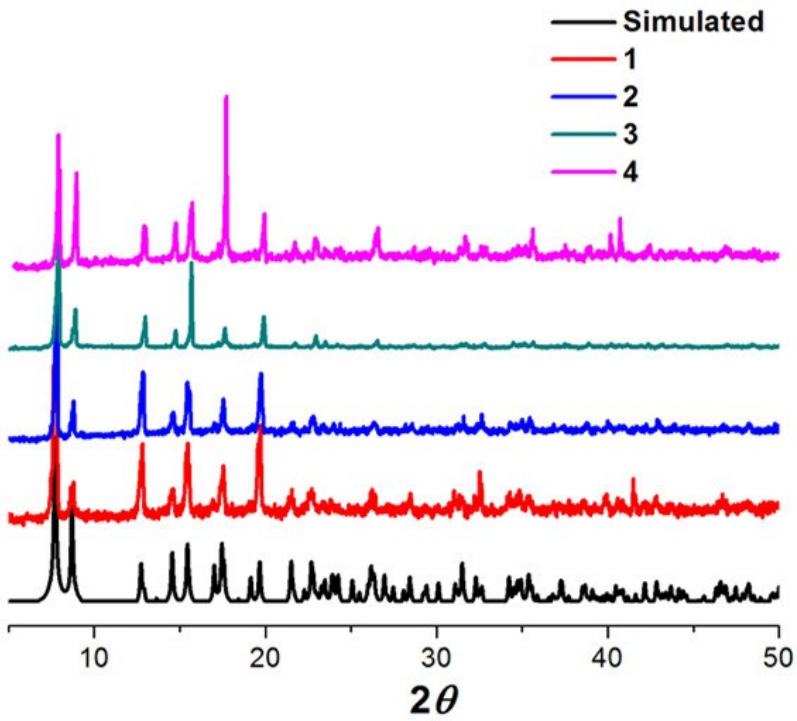

Fig. S3 Powder X-ray diffraction patterns of **1-4**.

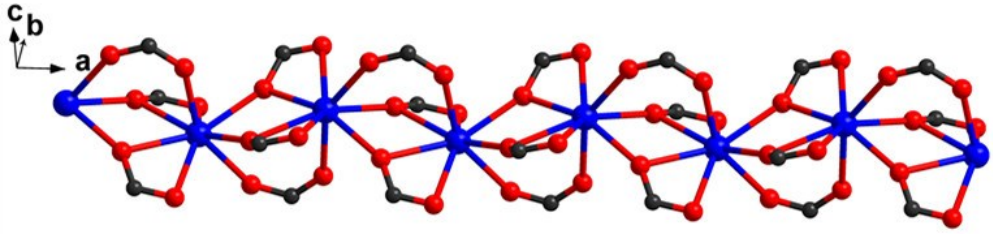

Fig. S4 The 1D chain-shaped building unit $[Gd(CO_2)_3]_n$ constructed from the adjacent Gd^{3+} ions and carboxyl groups of the HPAA ligands in **2**.

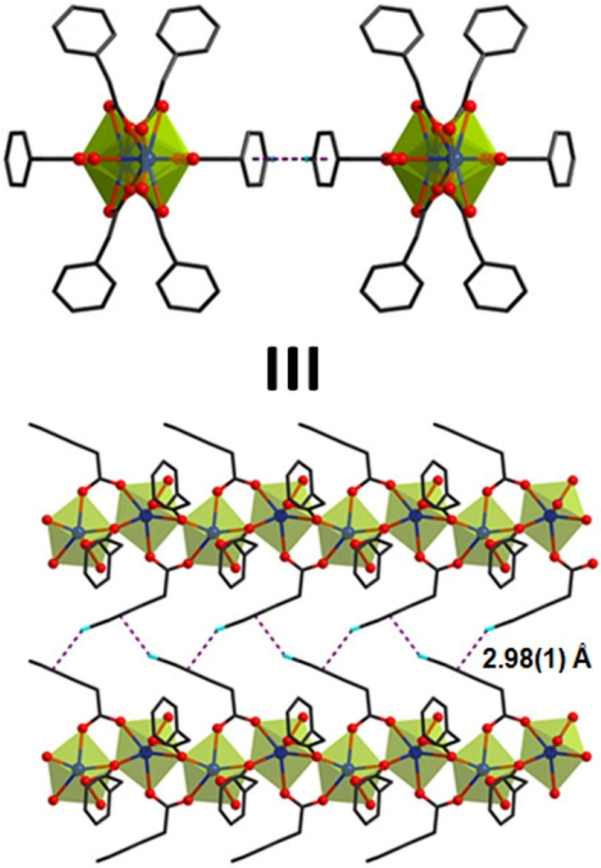

Fig. S5 View of the 2D supramolecular structure in **2** along *a* axis (top) and *b* axis (bottom) (C–H···π interaction: violet dotted lines).

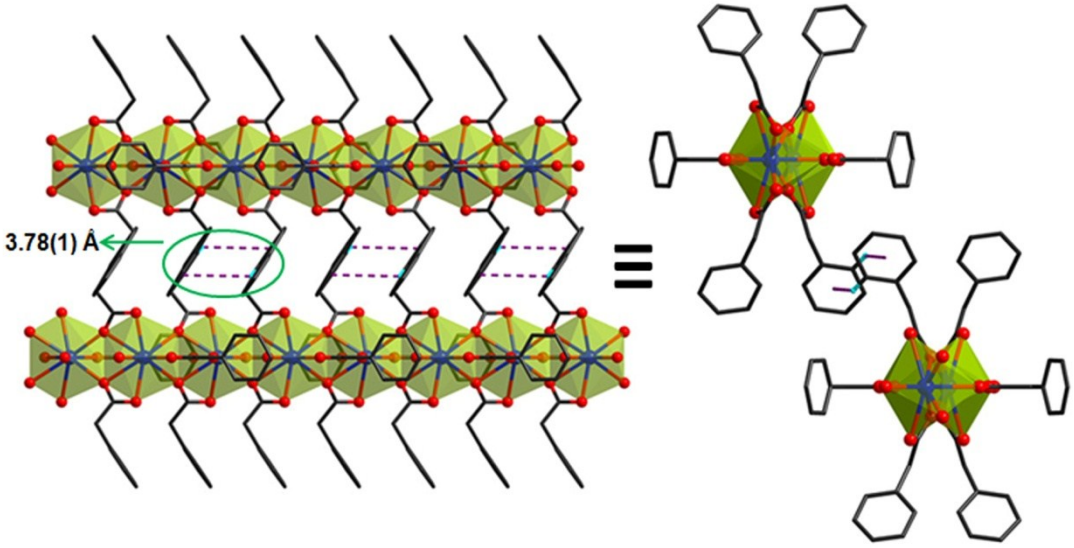

Fig. S6 View of the 2D supramolecular structure in **2** along *c* axis (left) and *a* axis (right) (C–H···π interaction: violet dotted lines).

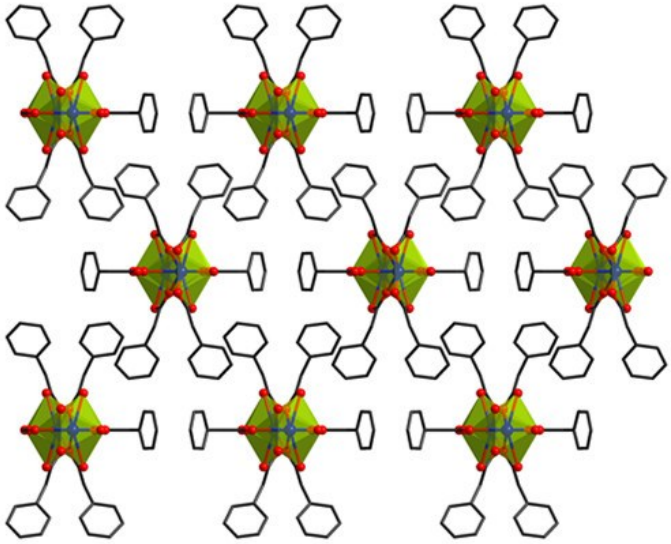

Fig. S7 Packing view of the 1D chains viewed along *a* axis. The C–H···π bonds have been omitted for clarity.

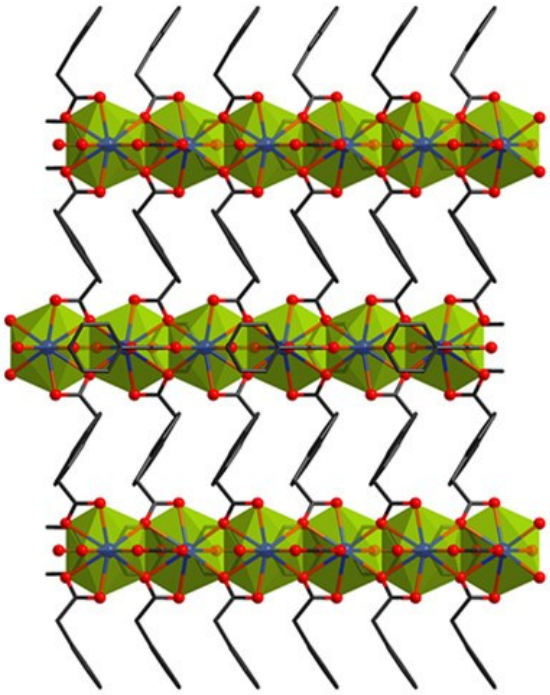

Fig. S8 Packing view of the 1D chains viewed along *c* axis. The C–H···π bonds have been omitted for clarity.

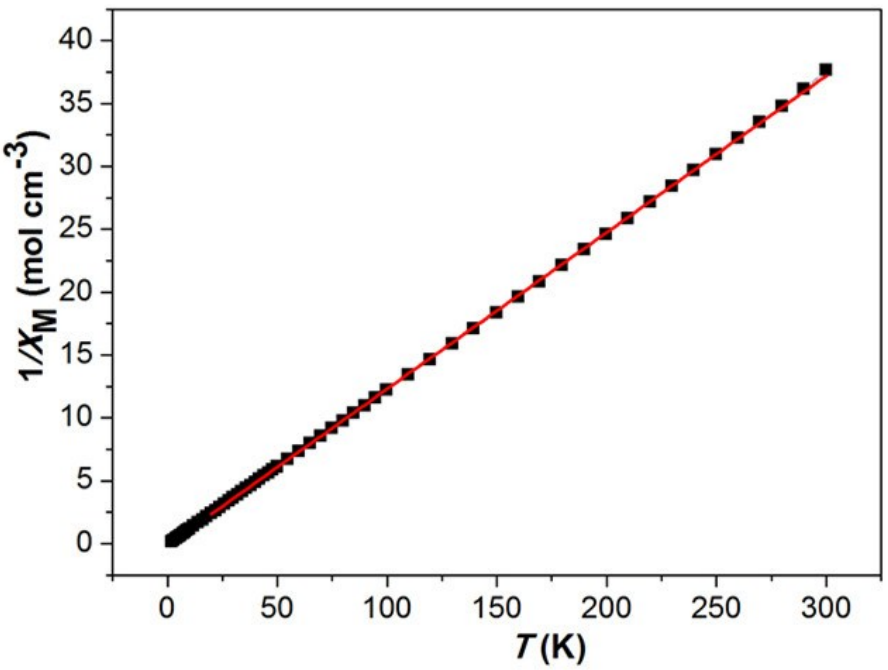

Fig. S9 Temperature dependence of the $1/\chi_M$ values for **2** at 1000 Oe dc magnetic field. The red solid line represents the best fit to the data between 20 and 300 K.

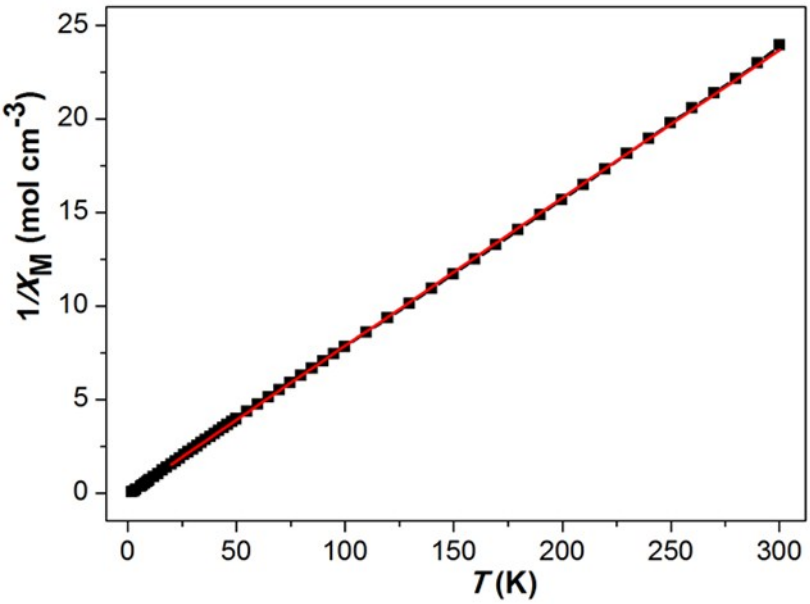

Fig. S10 Temperature dependence of the $1/\chi_M$ values for **3** at 1000 Oe dc magnetic field. The red solid line represents the best fit to the data between 20 and 300 K.

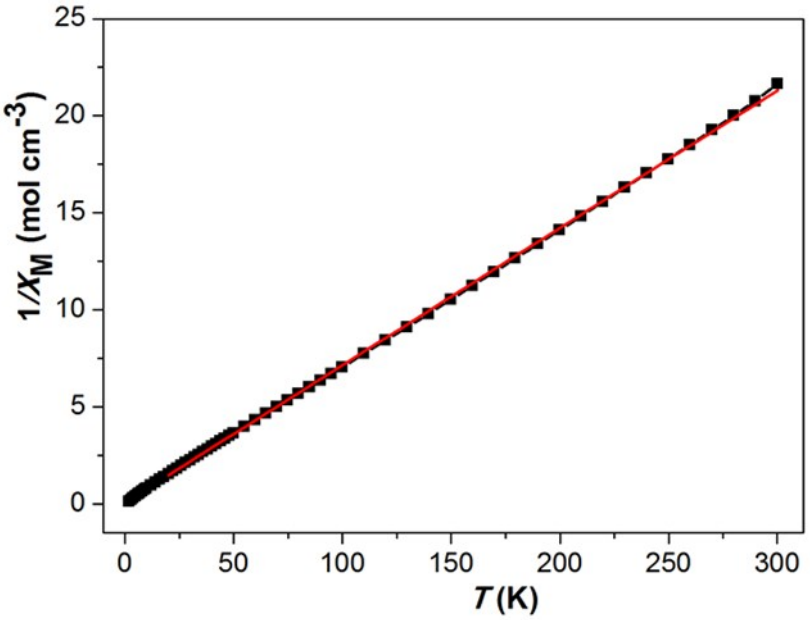

Fig. S11 Temperature dependence of the $1/\chi_M$ values for **4** at 1000 Oe dc magnetic field. The red solid line represents the best fit to the data between 20 and 300 K.

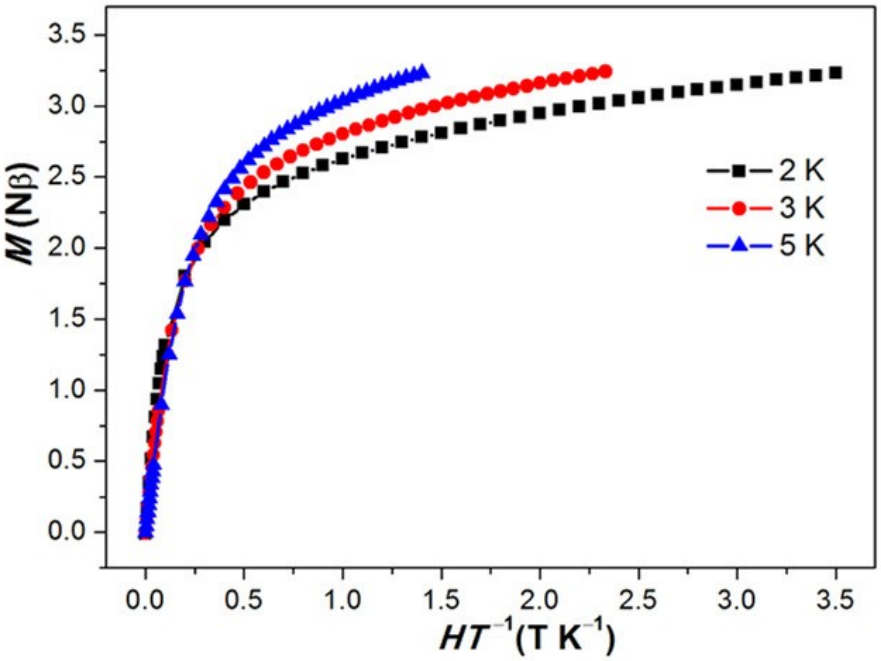

Fig. S12 *M* versus *H/T* plots at different temperatures for **4**.

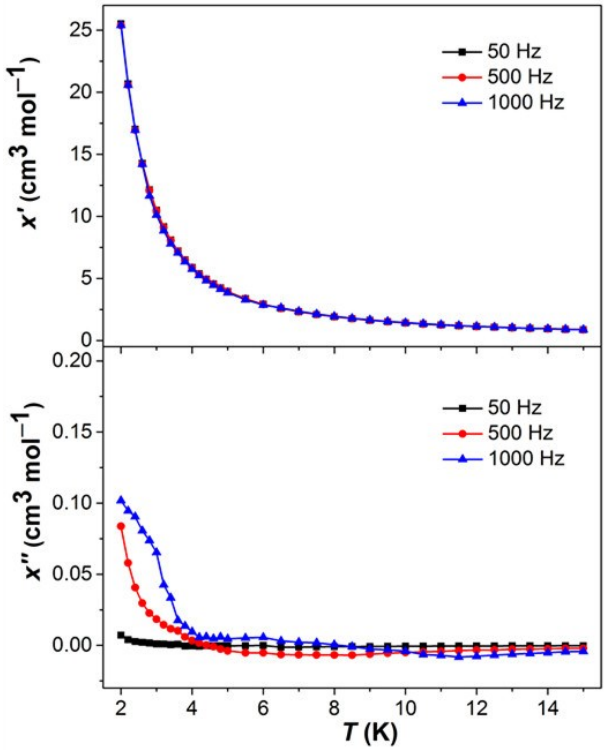

Fig. S13 Temperature dependence of the in-phase (χ′) and out-of-phase (χ″) ac susceptibility for **3** at the indicated frequencies and in the zero dc field.

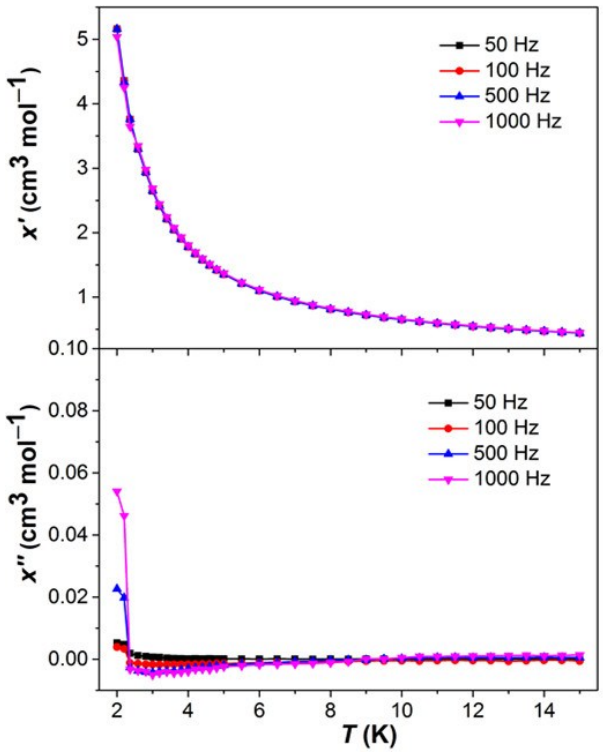

Fig. S14 Temperature dependence of the in-phase (χ′) and out-of-phase (χ″) ac susceptibility for **4** at the indicated frequencies and in the zero dc field.

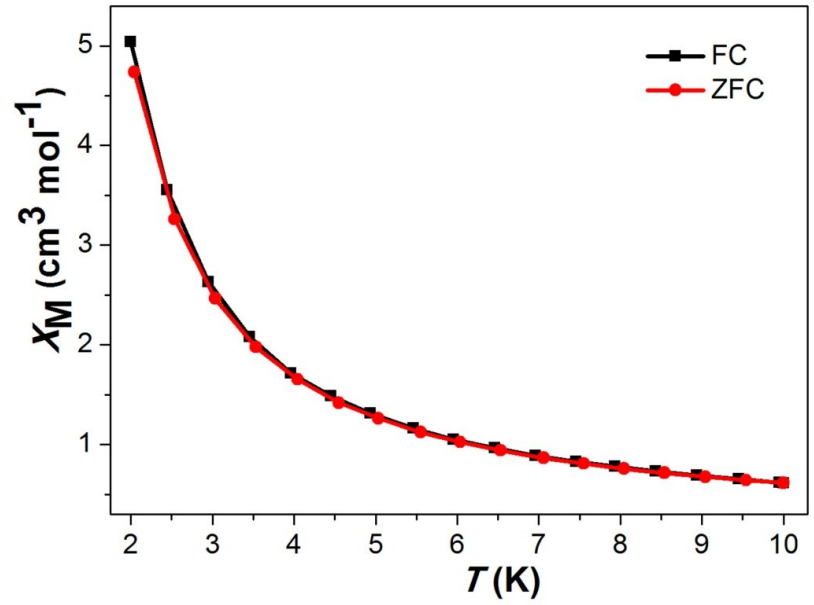

Fig. S15 FC and ZFC magnetization curves of **4** at 100 Oe.

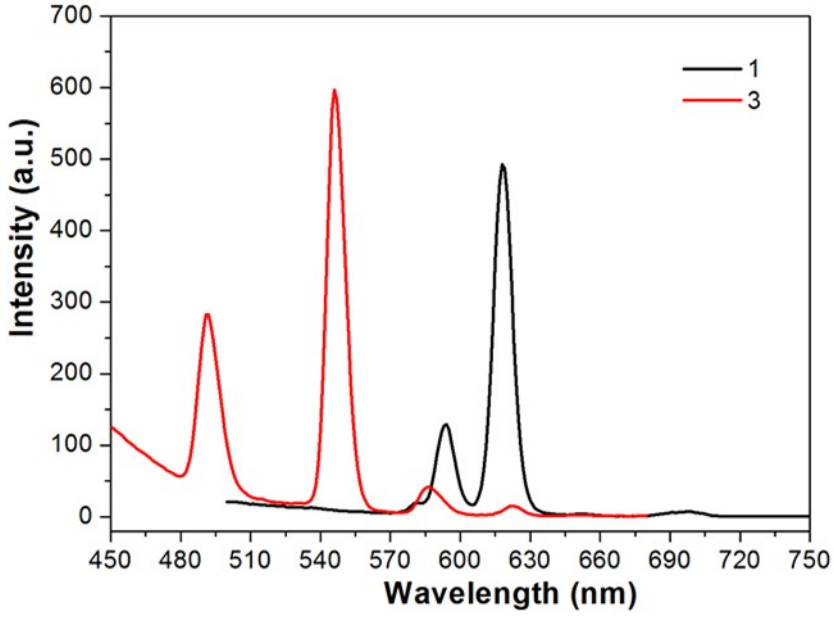

Fig. S16 The luminescence spectrum of **1** and **3** in DMF solution (10^{-3} mol L^{-1}), exited at 370 and 396 nm repectively.